Preparation and Structural Characterization of Two New Phases of Aluminum Trifluoride

Norman Herron,*,† David L. Thorn,† Richard L. Harlow,† Glover A. Jones,† John B. Parise,‡ Jaime A. Fernandez-Baca,§ and Thomas Vogt⊥

Central Research and Development Department, The DuPont Company,|| Wilmington, Delaware 19880-0328; Center for High Pressure Research, Earth and Space Sciences, State University of New York, Stoneybrook, New York 11794-2100; Solid State Division, Oak Ridge National Laboratory, Oak Ridge, Tennessee 37831; and Physics Department, Brookhaven National Laboratory, Upton, New York 11973-5000

Received September 22, 1994. Revised Manuscript Received November 9, 1994®

When certain salts, $R^+AlF_4^-$ are heated in flowing nitrogen, the equivalent of R^+F^- is lost at temperatures <500 °C, leaving microcrystalline AlF_3. This transformation proceeds via an intermediate material of formula $HAlF_4$ when R^+ = pyridineH^+ or occurs in a single step when, e.g., R^+ = an organic cation such as $N(CH_3)_4^+$. In each case a different, metastable phase of AlF_3 is produced and their structures, both based on corner-shared octahedra of [AlF_6], are delineated using powder diffraction (X-ray and neutron) techniques. When $HAlF_4$ is an intermediate, the ultimate η-AlF_3 phase has a structure identical to pyrochlore materials of formulae FeF_3 and $AlF_x(OH)_{3-x}$. When there is no discrete intermediate, the ultimate θ-AlF_3 phase has a structure which has now also been reported by Bentrup et al. During attempts to crystallize $HAlF_4$ from formamide, a new β-phase of NH_4AlF_4 was isolated and characterized by powder diffraction as a layered material having NH_4^+ ions between fluoroaluminate sheets and with connectivity within the sheets identical to the β-phase of $RbAlF_4$. The sheet structure loses NH_4F when pyrolyzed, producing yet another new phase, κ-AlF_3, which retains the connectivity of the layers from the precursor and simply fuses these layers together in a pseudotopotactic transformation. The resultant structure is closely related to that of the hypothetical end member of the tetragonal tungsten bronzes such as K_xWO_3 when $x = 0$. All three new phases contain [Al–F–Al] rings which dictate a limited nanoporosity and all convert irreversibly to the thermodynamically stable α-AlF_3 form at temperatures between ~450 and ~650 °C.

Introduction

In addition to commodity applications,[1] AlF_3 finds wide use as a catalyst in fluorochemicals manufacture, particularly in CFC and the new CFC-alternatives production.[2] This latter application is often dependent on the structural phase of the AlF_3 material[3] and has meant that much study and attendant folklore has evolved around the structural phase diagram of AlF_3 itself. Two phases are well characterized—α and β—with reliable synthetic and structural data available.[4,5] In both cases, the structures are built of octahedral [AlF_6] units where all of the fluoride ions are corner-shared. The patent literature is replete with a litany of other less-substantiated claims to additional phases (e.g., γ, δ, ϵ) which may represent either impure materials or mixtures of the better characterized phases.[2,6] Our previous preparation[7] of organic cation salts with fluoroaluminate anions of stoichiometry $R^+AlF_4^-$ provides a potential new route to aluminum fluoride phases. Pyrolysis of such salts is expected to evolve the equivalent of R^+F^-, leaving behind AlF_3, and this transformation may be detected quantitatively by TGA.

The definitive preparations and structural characterizations of two previously unknown phases of AlF_3 as well as two new intermediate precursors of AlF_3 are now reported with their attendant thermal behaviors.

Experimental Section

The precursor, organic cation salts of general stoichiometry $M^+AlF_4^-$ were prepared according to the procedures of ref 7. All sample handling was performed under a dry nitrogen atmosphere in a glovebox, and samples for diffraction studies were loaded into containers under nitrogen wherever possible. All solvents were nitrogen purged and dried over 4A molecular sieves before use. Thermogravimetric analysis (TGA) of the precursor salts was performed with a TA Instruments/DuPont 951 TGA apparatus. The conversions of the various precursors

† The DuPont Co.
‡ State University of New York.
§ Oak Ridge National Laboratory.
⊥ Brookhaven National Laboratory.
|| DuPont Contribution No. 6541.
® Abstract published in *Advance ACS Abstracts,* December 15, 1994.

(1) Cochet-Muchy, B.; Portier, J. In *Inorganic Solid Fluorides, Chemistry and Physics;* Hagenmuller, P., Ed.; Academic Press: Orlando, FL, 1985; p 580.
(2) Christoph, F. J.; Teufer, G. U.S. Patent 3,178,484, 1965. Christoph, F. J.; Teufer, G. G.B. Patent 1,026,105, 1966.
(3) Corbin,D. R.; Rao, V. N. M. WO 92/16479 (1992) to E. I. du Pont de Nemours and Co., Inc.
(4) Hoppe, R.; Kissel, D. *J. Fluorine Chem.* **1984,** *24,* 327. Daniel, P.; Bulou, A.; Rousseau, M.; Nouet, J.; Fourquet, J. L.; Leblanc, M.; Burriel, R. *J. Phys: Condensed Matter* **1990,** 2:5663.
(5) Le Bail, A.; Jacoboni, A.; Leblanc, M.; DePape, R.; Duroy, H.; Fourquet, J. L. *J. Solid State Chem.* **1988,** *77,* 96–101.
(6) Christoph, F. J.; Teufer, G. U. S. Patent 3,178,483, 1965. Shinn, D. B.; Crocket, D. S.; Haendler, H. M. *Inorg.Chem.* **1966,** *5,*1927. Bulou, A.; Leble, A.; Hewat, A. W.; Fourquet, J. L. *Mater. Res. Bull.* **1982,** *17,* 391. Jouanneaux, A.; Leble, A.; Pannetier, J.; Fourquet, J. L. *J. Phys.: Condens. Matter* **1989,** *1,* 1577.
(7) Herron, N.; Thorn, D. L.; Harlow, R. L.; Davidson, F. *J. Am. Chem. Soc.* **1993,** *115,* 3028.

0897-4756/95/2807-0075$09.00/0

into the new phases of $HAlF_4$ and AlF_3 were followed by TGA under flowing (150 mL/min) nitrogen by ramping at 10 °C/min to 900 °C. Conversion of the new phases of AlF_3 into α-AlF_3 was followed by *in situ* powder X-ray diffraction (XRD) as well as differential scanning calorimetry (DSC) using a TA Instruments DSC cell under nitrogen purge. Surface area estimates for the new phases of AlF_3 were made using standard five-point BET isotherm measurements using nitrogen gas adsorption. In-house X-ray diffraction spectra for preliminary identification of phase behavior were collected on a Philips APD3720 powder diffractometer using Cu Kα radiation. Elemental analysis was performed by Galbraith Inc, Knoxville TN.

Synthesis of New Materials. *$HAlF_4$*: The material pyridineH·AlF_4[7](5 g) is loaded as a shallow bed into a quartz boat in a quartz-lined tube furnace having a flowing nitrogen atmosphere (200 mL/min). The exhaust nitrogen from the tube will contain pyridine and must be vented to a suitable hood system or scrubbed appropriately. The temperature is then ramped to 225 °C at 10 °C/min and then held at 225 °C for 30 min. The material is then cooled in the nitrogen flow and collected for characterization by XRD with major diffraction peaks at *d* spacings of 10.30, 5.13, 4.03, 3.83, 3.49, 3.11, and 2.04 Å (see supplementary material). Yield is quantitative, ~2.85 g.

η-AlF_3: Repeating the procedure reported above for $HAlF_4$ except ramping to a top temperature of 370 °C evolves pyridine and then HF with production of the η-AlF_3 phase in quantitative yield. XRD reveals major diffraction peaks at *d* spacings of 5.56, 2.90, 2.78, 1.97, 1.86, 1.71, and 1.63 Å.

θ-AlF_3: The material $N(CH_3)_4AlF_4$[7] (5.0 g) is placed in a quartz boat in a horizontal tube furnace lined with a quartz liner. Air is passed through the tube and vented to an efficient hood system at 200 mL/min. As the temperature is ramped to 450 °C at 10 °C/min, white sublimate begins to collect on the cool exit end of the quartz liner tube. The sample is held at 450 °C for 30 min and then cooled and collected. Yield of AlF_3 is essentially quantitative and phase purity can be checked by XRD with major diffraction peaks at *d* spacings of 5.89, 5.11, 4.17, 3.86, 3.61, 3.39, 3.22, 3.08, and 2.94 Å (see supplementary data for details of diffraction pattern).

β-NH_4AlF_4: The material pyridineH·AlF_4[7] (5.0 g) is slurried into 10 mL of dry formamide in a nitrogen filled glovebox. After slight warming and stirring, the solid dissolves to give a clear colorless solution. The solution is then rapidly heated in an open container with stirring until at ~180 °C vigorous fizzing and boiling occurs. At this point an opalescent white precipitate begins to form quickly and after ~1 min the heat is removed from the solution and it is allowed to cool slowly to room temperature. A dense white precipitate forms during cooling and is collected by filtration, washed with formamide, and suction dried to a microcrystalline white powder, yield ~2.8 g (85%). Anal. Calcd for NH_4AlF_4: H 3.33; N 11.57; F 62.8; Al 22.3%. Found: H 3.21; N 11.57; F 62.3; Al 22.7%.

κ-AlF_3: The solid β-NH_4AlF_4 (5.0 g) prepared as described above is loaded into a quartz boat and placed in a quartz lined horizontal tube furnace equipped with a nitrogen purge (200 mL/min). The exit stream is vented to an efficient hood system as the temperature is ramped to 450 °C at 10 °C/min. A white sublimate collects on the cool exit end of the liner tube. The sample is held at 450 °C for 4 h and then cooled to room temperature in the flowing nitrogen. The phase purity of the resultant AlF_3 (yield is essentially quantitative) is checked by XRD with major diffraction peaks at *d* spacings of 5.09, 3.61, 3.54, and 3.17 Å (see Figure 1 for details of diffraction pattern).

Details of the Structural Refinements. *η-AlF_3*: A powder sample of η-AlF_3 was compressed into a deep flat plate holder and data were collected in high resolution mode[8] at the X7a beamline at the National Synchrotron Light Source, Brookhaven National Laboratory. The beamline was configured with a Si(111) monochromator and Ge(220) analyzer, a Kevex detector and incident beam-defining slits of 8.0 mm by 0.8 mm. The wavelength, calibrated using an Si powder standard with a = 5.430 825 Å, was 0.699 39(2) Å. The data were collected in two scans, from 5 to 30° and from 30 to 64° in 2θ with a step size of 0.01° and counting times of 4 and 6 s, respectively. Perusal of the X-ray powder diffractogram indicated that all peaks could be explained by either the face centered cubic unit cell with a = 9.62 Å for η-AlF_3, or by that of the published data for β-AlF_3. Structure refinement using GSAS (Larsen, A. C.; Von Dreele, R. B. *LANSCE* **1990**) was initiated using the atomic positions given in ref 9 for the hydroxy analogue of η-AlF_3. Several cycles of least squares lead to convergence. Refinement of the anisotropic model for thermal motion lead to an essentially isotropic result and so was not pursued. Those regions contaminated by impurity phases were excluded from the refinement. Crystallographic information is in Table 1.

θ-AlF_3: The X-ray structural data for θ-AlF_3 were collected on the same instrument used for the η-phase except that the wavelength used was 0.700 59(3) Å, the 2θ range was 5–60°, the step size was 0.005°, the count time was 4 s, and the

(8) Cox, D. E.; Toby, B. H.; Eddy, M. M. *Aust. J. Phys.* **1988**, *41*, 117.

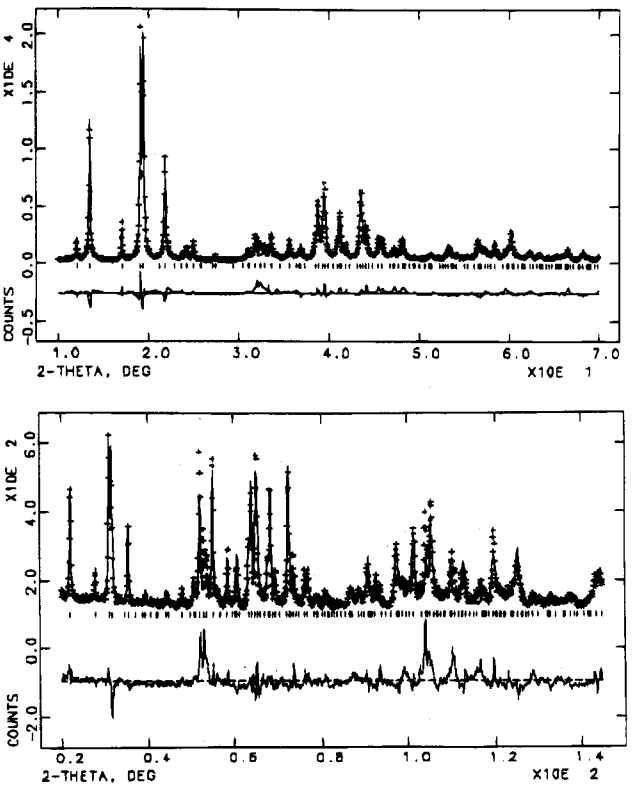

Figure 1. Results of the (a) X-ray, 1.1976 Å, and (b) neutron, 1.8857 Å, refinements of κ-AlF_3. Observed (+) and calculated (line) intensities are plotted, while the difference intensity is plotted below the tick marks.

Table 1. Crystallographic Information

compound	η-AlF_3	θ-AlF_3	β-NH_4AlF_4	κ-AlF_3
crystal system	cubic	tetragonal	tetragonal	tetragonal
space group	*Fd3m*	*P4/nmm*	*I4/mcm*	*P4/mbm*
Z	16	16	20	10
cell parameters:				
a, Å	9.6225(1)	10.1844(1)	11.6390(1)	11.4033(4)
c		7.1728(1)	12.6602(3)	3.5436(1)
V, Å^3	890.97	743.98	1715.03	460.79
density, g cm^{-3}	2.504	2.999	2.343	3.026
wavelength:				
X-ray, Å	0.69939(2)	0.70059(3)	0.80063(2)	1.19759(4)
neutron, Å		1.4163(1)		1.8857(1)
Two-θ range:				
X-ray, deg	5–64	5–60	5–47	10–70.5
neutron, deg		11–135		18–155
R, X-ray/neutron	0.050	0.054/0.047	0.133	0.111/0.140
R_p	0.122	0.091/0.033	0.111	0.171/0.123
R_{wp}	0.097	0.128/0.038	0.146	0.123/0.093

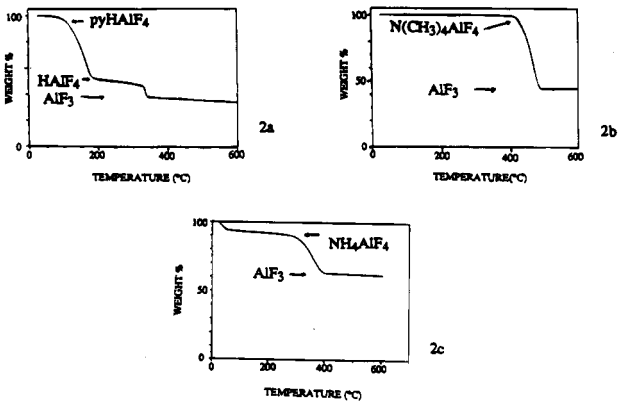

Figure 2. Thermogravimetric analysis curves of (a) pyridineH·AlF_4·0.48pyridine, (b) $N(CH_3)_4AlF_4$, and (c) β-NH_4AlF_4. Plots are generated by monitoring the sample weight as a function of temperature in flowing nitrogen (150 mL/min) and at a temperature ramp of 10 °C/min. Stoichiometries calculated from the weight change data are indicated on the curves.

sample was both rocked and spun. Although indexing the pattern was quite straightforward yielding a tetragonal unit cell with a = 10.1844(1) and c = 7.1728(1) Å, manual deconvolution of the highly overlapped peaks ($c \cong a/\sqrt{2}$, plus the presence of other AlF_3 phases) was found to be necessary in order to correctly assign the intensities from each set of planes. The space group was clearly primitive and an n-glide perpendicular to the unique axis was indicated: space group *P4/nmm* was thus assigned. Direct methods eventually succeeded in solving the structure but only after some manual intervention in the phasing process. The neutron diffraction data were collected using the HB4 high-resolution powder diffractometer at the high flux isotope reactor at Oak Ridge National Laboratory. This instrument has a Ge(115) monochromator; the neutron wavelength was determined to be 1.4163 Å from the Rietveld refinement of nickel and silicon powder standards. Soller-slit collimators of 12 and 20 ft are positioned before and after the monochromator crystal. A bank of 32 equally spaced (2.7° apart) He-3 detectors, each with a 6 ft collimator, were step-scanned over a 40° range to provide a diffraction pattern between 11 and 135°. The sample was placed in a vanadium can which was rotated at 6 rpm during the data collection in order to reduce possible preferred orientation effects. Each intensity in the diffraction pattern was obtained from the average from a number of detectors (this number reaches a maximum of 15 in the central part of the pattern). The intensities shown have been normalized to 3 min/step.

The refinement of the structure using both the X-ray and neutron data by the Rietveld method (GSAS) was straightforward, although the β- and η-AlF_3 phases appeared as minor constituents, 4.7(4) and 4.9(8)% of the sample, and needed to be added to the structure factor calculation as fixed contributors although the scale factors and peak profiles for these contaminant phases were refined. Parameters for the β-AlF_3 phase were taken from ref 5. Crystallographic information is in Table 1.

β-NH_4AlF_4: The X-ray data for the β-phase of ammonium aluminum fluoride were collected at the NSLS on the new powder diffraction beamline, X3b1. Although physically smaller than X7a's diffractometer, it was similarly configured. The ab initio structural solution was conducted in the same manner as that of the θ phase of AlF_3. During the refinement of the structure, however, the isotropic thermal parameters of the two nitrogen atoms went negative (ca. −0.02). Since the hydrogen atoms attached to the nitrogens must be disordered and since they could not be located in a difference-density map, the occupancies of the nitrogen atoms were allowed to vary. Both occupancies rose to approximately 1.5 (theoretical for a disordered NH_4 cation would be $^{11}/_7 = 1.57$), while the isotropic thermal parameters also became quite large. Since the quality of the overall refinement improved considerably using this model, the refinement was stopped at this point. It should be pointed out, however, that there were many attempts to include disordered hydrogen atoms—none of these refinements converged in a reasonable fashion but all improved the thermal parameter problem of the nitrogen atoms. The quality of the data was checked by substituting in-house X-ray data for the synchrotron data; still the nitrogen atoms went "negative". Chemical analysis also clearly showed that the compound contained ammonium and not sodium, for example, which could also have accounted for the negative thermal parameters. Crystallographic information is listed in Table 1. Possible noncentrosymmetric space groups *I4cm* and *I$\bar{4}$c2* were not used to refine this structure because the fit in the centrosymmetric structure was quite good. The only problem with the structure, the low thermal parameters of the nitrogen atoms, is the opposite of what one would expect if the sites in the centrosymmetric structure were actually "averaged" positions from a noncentrosymmetric structure.

κ-AlF_3: The X-ray data for the κ phase were again collected at X7a. Although the structure was solved by the ab initio method, it probably could have been solved by inspection of the individual layers in the parent compound, β-NH_4AlF_4, plus a little imagination (basically, the two structures contain the same layers in somewhat different orientations). The refinement of the structure using only the X-ray data appeared straightforward although the differences in the thermal parameters of chemically equivalent atoms and some small differences between the observed and calculated patterns were cause for concern (see Figure 1a). A neutron pattern was then obtained from the powder line BT-1 at NIST; it showed that the background was quite high and strongly suggested that not all of the hydrogen had been removed from the sample under the decomposition conditions. A second sample was then prepared using a long annealing time. It was sent to

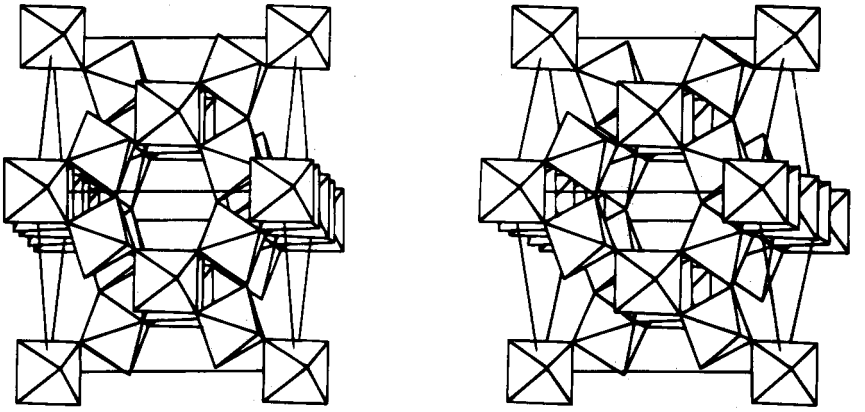

Figure 3. Stereodrawing of the η-AlF_3 structure (polyhedral representation) looking nearly parallel to the [110] direction to show the channels which run through the crystal. Bond length: Al−F, 1.803(1) Å. Bond angles: *cis* F−Al−F, 89.8(1)° and 90.2(1)°; Al−F−Al, 141.3(1)°.

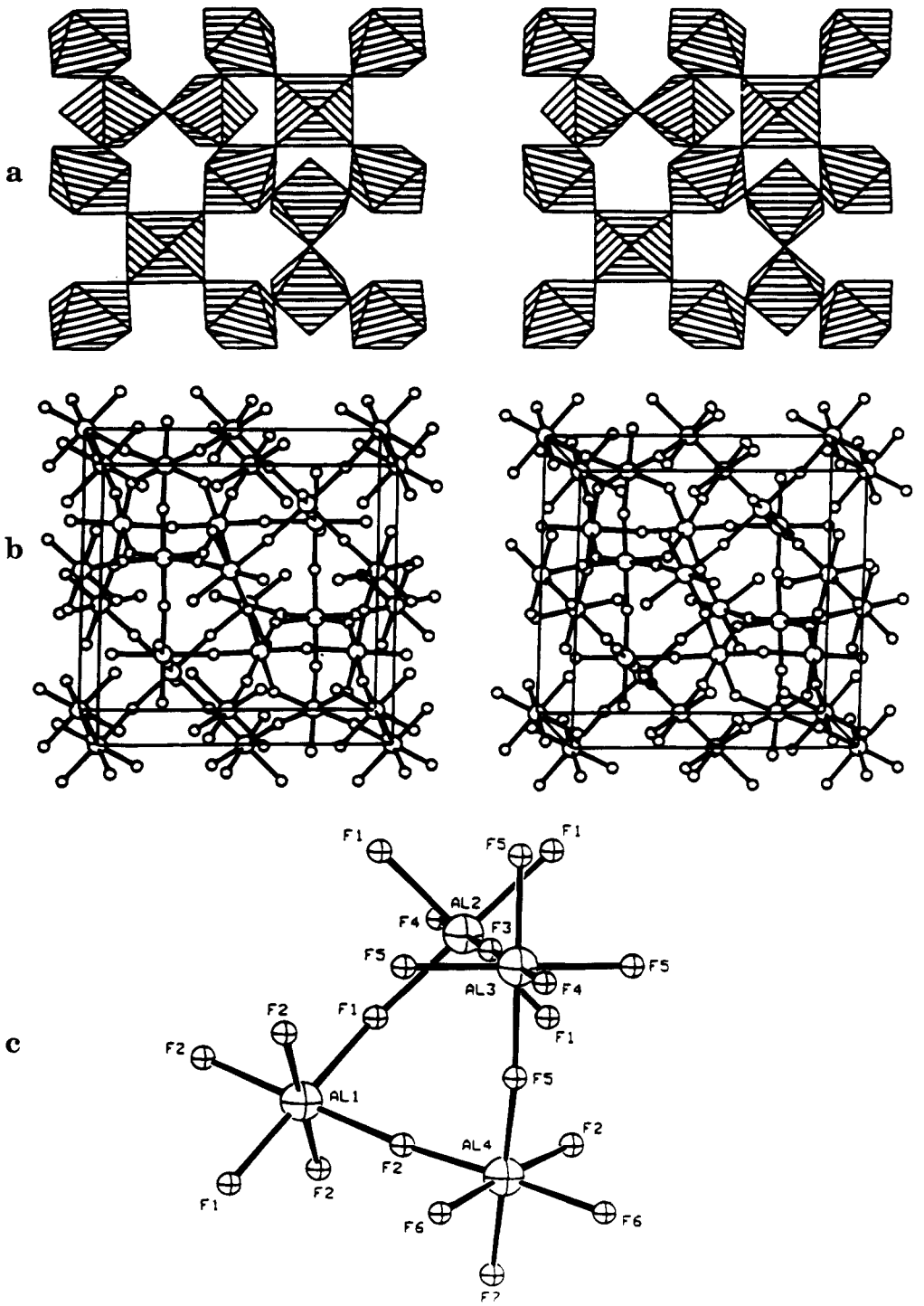

Figure 4. (a) Stereoview of a single "layer" (polyhedral representation) of θ-AlF_3 emphasizing the 4- and 5- rings of the linked [AlF_6] octahedra. (b) Stereoview of the θ-AlF_3 structure (ball and stick representation) nearly parallel to the c axis of its tetragonal cell. (c) The atom labeling scheme for θ-AlF_3.

the new high-resolution neutron powder diffractometer (HRNPD) at the high flux beam reactor (HFBR) at Brookhaven National Laboratory (this beamline configuration is described in full in: Passell, L.; Bar-ziv, S.; Gardner, D. W.; Cox, D. E.; Axe, J. D. A New High Resolution Neutron Powder Diffractometer at the Brookhaven High Flux Beam Reactor. *Mater. Sci. Forum* **1991**, *79*−82, 475−480). The refinement was then continued using both data sets. The fit between the observed and calculated intensities for the neutron pattern was actually worse than for the X-ray data (see Figure 1b). In an attempt to resolve this difference, many aspects of the structure were reviewed. First, the patterns of the other known AlF_3 phases were checked; no matches were found. Second, the unit cell was expanded in both a and c, but several clearly observable peaks could still not be fit. Third, difference maps were examined closely for "trapped" atoms within the structure's pores; even when the peaks made chemical sense, the atoms failed to refine with meaningful occupancies. Hydrogen atoms were particularly sought because of their stronger contribution to the neutron pattern than to the x-ray pattern. Although the background of the neutron pattern suggested that some hydrogen might be present (even after the long annealing), an infrared spectrum of the sample showed no peaks attributable to hydrogen (H−F or F−H−F hydrogen-bonded species). At the end of this investigation, it was concluded that the difference between the observed and calculated intensities is probably due to one of two effects: (1) the existence of yet another AlF_3 phase of unknown structure and/or (2) the presence of interlayer stacking faults, particularly along the c axis, introduced during the reorganization necessary to

realign the layers of the precursor β-NH_4AlF_4 into the κ-phase. Whatever the cause, its presence has undoubtedly limited the accuracy of the refinement, particularly the thermal motions. Crystallographic details are listed in Table 1.

When refinements of the κ-AlF3 structure in the centrosymmetric space group led to a poor fit between the observed and calculated intensities, attempts were made to refine the structure in both *P4bm* and *P4̄b2*. Neither space group improved the overall fit, although in *P4̄b2* certain specific large differences were reduced. Both refinements were "unstable" in the sense that they produced very unusual geometries around the Al atoms. Electron diffraction of the sample has suggested that the unit cell is correct despite the occurrence of "extra" peaks in the X-ray and neutron patterns. We are still looking for impurity phases by TEM but have not found any so far. Whatever these peaks are due to (impurity phase, stacking faults, etc.), the refinement in all of the space groups attempts to fit some of this extra intensity—the more variables, the better the fit. Because of this problem, there was a need to stop at some reasonable point when as much information as possible had been extracted from the patterns. The centrosymmetric structure clearly represents the best that could be done with the present data. It may well be an approximation and the real structure may be a perturbation of this model.

Results and Discussion

(1) η-AlF_3. In the case $R^+AlF_4^-$, when R^+ is the pyridinium cation, $C_5H_5NH^+$, the solid recovered from the initial preparation is typically contaminated with excess pyridine solvent.[7] This excess pyridine is difficult to remove cleanly given the ready decomposition of pyridineH·AlF_4, and so we have worked with materials commonly containing 0–50% excess of pyridine over that dictated by the molecular stoichiometry. In such cases, heating first evolves pyridine at ~100–150 °C (both the excess and the stoichiometric pyridine evolve almost simultaneously) leaving a crystalline material of stoichiometry $HAlF_4$ (see below). At 325 °C a clean evolution of HF from this material leaves pure AlF_3 with no further weight changes occurring up to 900 °C (see Figure 2a). (TGA-MS and TGA-IR confirm that *only* pyridine is lost in the first thermal event and *only* HF in the second.) X-ray diffraction (XRD) patterns of the final material reveal it to be phase-pure α-AlF_3 having no contamination from corundum Al_2O_3. The microcrystalline material produced immediately after the loss of HF from the $HAlF_4$ intermediate has an XRD pattern showing a small component of poorly crystalline β-AlF_3 but revealing a major crystalline phase reminiscent of the known pyrochlore materials $AlF_x(OH)_{3-x}$ ($0.4 < x < 2.07$)[9] and FeF_3.[10] The fact that no further weight changes or crystalline Al_2O_3 phases are detected upon heating to 900 °C prove that, in this case, $x = 3$.[9] A pure AlF_3 material having this structure has never been reported, and so we have refined the structure of this compound using XRD data and Rietveld techniques. The new phase is designated η-AlF_3, and its structure refines well using the B_2X_6 framework pyrochlore model.[11] The structure is depicted in Figure 3 and can be viewed as a relative of the established β-AlF_3 phase having the same nanoporous openings defined by corner-shared rings of six [AlF_6] octahedra. However, whereas the β-phase material has these openings aligned throughout the crystal to form straight channels along [001],[5] the η-phase has adjacent rings tilted with respect to each other producing an undulating channel along [110] of approximate diameter 2.6 Å. This undulation is imposed by the other key structural feature of the pyrochlore framework structure—the presence of clusters of four tetrahedrally disposed [AlF_6] octahedra as defined by the B_2X_6 diamond-net of the base structure type.[11] Three fluoride ions from each of the four octahedra in the cluster are corner-shared to the other three octahedra of the cluster.

Table 2

(a) Positional and Isotropic Thermal Parameters for θ-AlF_3

atom[a]	multiplicity, Wyckoff letter, site sym	X	Y	Z	U_{iso}
Al(1)	4 d ..2/*m*	0.0	0.0	0.0	0.0071(4)
Al(2)	2 c 4*mm*	0.25	0.25	−0.0932(4)	0.0077(6)
Al(3)	2 c 4*mm*	0.25	0.25	0.4137(4)	0.0074(7)
Al(4)	8 i .*m*.	0.25	−0.0862(1)	0.3274(2)	0.0070(3)
F(1)	8 j ..*m*	0.1208(1)	0.1208(1)	−0.0923(3)	0.0075(5)
F(2)	16 k 1	0.1223(1)	−0.0522(1)	0.1610(2)	0.0102(4)
F(3)	2 c 4*mm*	0.25	0.25	0.1573(6)	0.0119(11)
F(4)	2 c 4*mm*	0.25	0.25	−0.3355(6)	0.0106(11)
F(5)	8 i .*m*.	0.25	0.0770(2)	0.4130(3)	0.0098(6)
F(6)	8 h ..2	0.1262(1)	−0.1262(1)	0.5	0.0111(6)
F(7)	4 f 2*mm*	0.25	−0.25	0.2433(5)	0.0070(8)

(b) Bond Distances (Å) and Angles (deg) for θ-AlF_3

Al(1)–F(1)	1.862(2)	Al(3)–F(4)	1.799(6)
Al(1)–F(2)	1.780(2)	Al(3)–F(5)	1.762(3)
Al(2)–F(1)	1.861(2)	Al(4)–F(2)	1.799(2)
Al(2)–F(3)	1.796(5)	Al(4)–F(5)	1.772(3)
Al(2)–F(4)	1.738(5)	Al(4)–F(6)	1.813(1)
Al(3)–F(3)	1.839(5)	Al(4)–F(7)	1.774(2)
F(1)–Al(1)–F(1)	180.00	F(4)–Al(3)–F(5)	90.15(12)
F(1)–Al(1)–F(2)	88.03(6)	F(5)–Al(3)–F(5)	90.00
F(1)–Al(1)–F(2)	91.97(6)	F(5)–Al(3)–F(5)	179.71(1)
F(2)–Al(1)–F(2)	180.00	F(2)–Al(4)–F(2)	92.62(11)
F(2)–Al(1)–F(2)	89.80(10)	F(2)–Al(4)–F(5)	92.81(8)
F(2)–Al(1)–F(2)	90.20(10)	F(2)–Al(4)–F(6)	89.62(6)
F(1)–Al(2)–F(1)	90.00	F(2)–Al(4)–F(6)	177.35(10)
F(1)–Al(2)–F(1)	179.61(1)	F(2)–Al(4)–F(7)	87.46(10)
F(3)–Al(2)–F(4)	180.00	F(2)–Al(4)–F(5)	92.81(8)
F(1)–Al(2)–F(3)	89.80(10)	F(5)–Al(4)–F(6)	88.51(9)
F(1)–Al(2)–F(4)	90.20(10)	F(5)–Al(4)–F(7)	179.61(1)
F(3)–Al(3)–F(4)	180.00	F(6)–Al(4)–F(6)	88.12(11)
F(3)–Al(3)–F(5)	89.85(12)	F(6)–Al(4)–F(7)	91.21(9)
Al(1)–F(1)–Al(2)	159.4(1)	Al(3)–F(5)–Al(4)	159.9(2)
Al(1)–F(2)–Al(4)	173.7(1)	Al(4)–F(6)–Al(4)	141.1(2)
Al(2)–F(3)–Al(3)	180.00	Al(4)–F(7)–Al(4)	140.2(2)
Al(2)–F(4)–Al(3)	180.00		

[a] See Figure 4c for labeling scheme.

(2) θ-AlF_3. When the material $R^+AlF_4^-$ has $R^+ = N(CH_3)_4^+$,[12] the thermal behavior of the salt is quite different from that of the pyridinium salt detailed above. A single weight-loss event at 450 °C corresponds exactly to loss of the equivalent of "$N(CH_3)_4F$". The product AlF_3 shows no further weight loss up to 900 °C (Figure 2b) at which point it is easily identified by XRD as α-AlF_3. The product formed immediately after the weight-loss feature has a diffraction pattern showing a very small contamination by α-, β- and η-AlF_3 but with a major crystalline phase which could not be matched

(9) Cowley, J. M.; Scott, T. R. *J. Am. Chem. Soc.* **1948**, *70*, 105–109. Fourquet,J. L.; Riviere, M.; Le Bail, A.; Nygrens. M.; Grins, J. *Eur. J. Solid State Inorg. Chem.* **1988**, *25*, 535.

(10) DePape, R; Ferey, G. *Mater. Res. Bull.* **1986**, *21*, 971–978.

(11) Wells, A. F. In *Structural Inorganic Chemistry*, 5th ed.; Clarendon Press: Oxford 1986; p 258.

(12) Herron, N.; Thorn, D. L.; Harlow, R. L. *Inorg. Chem.* **1993**, *32*, 2985.

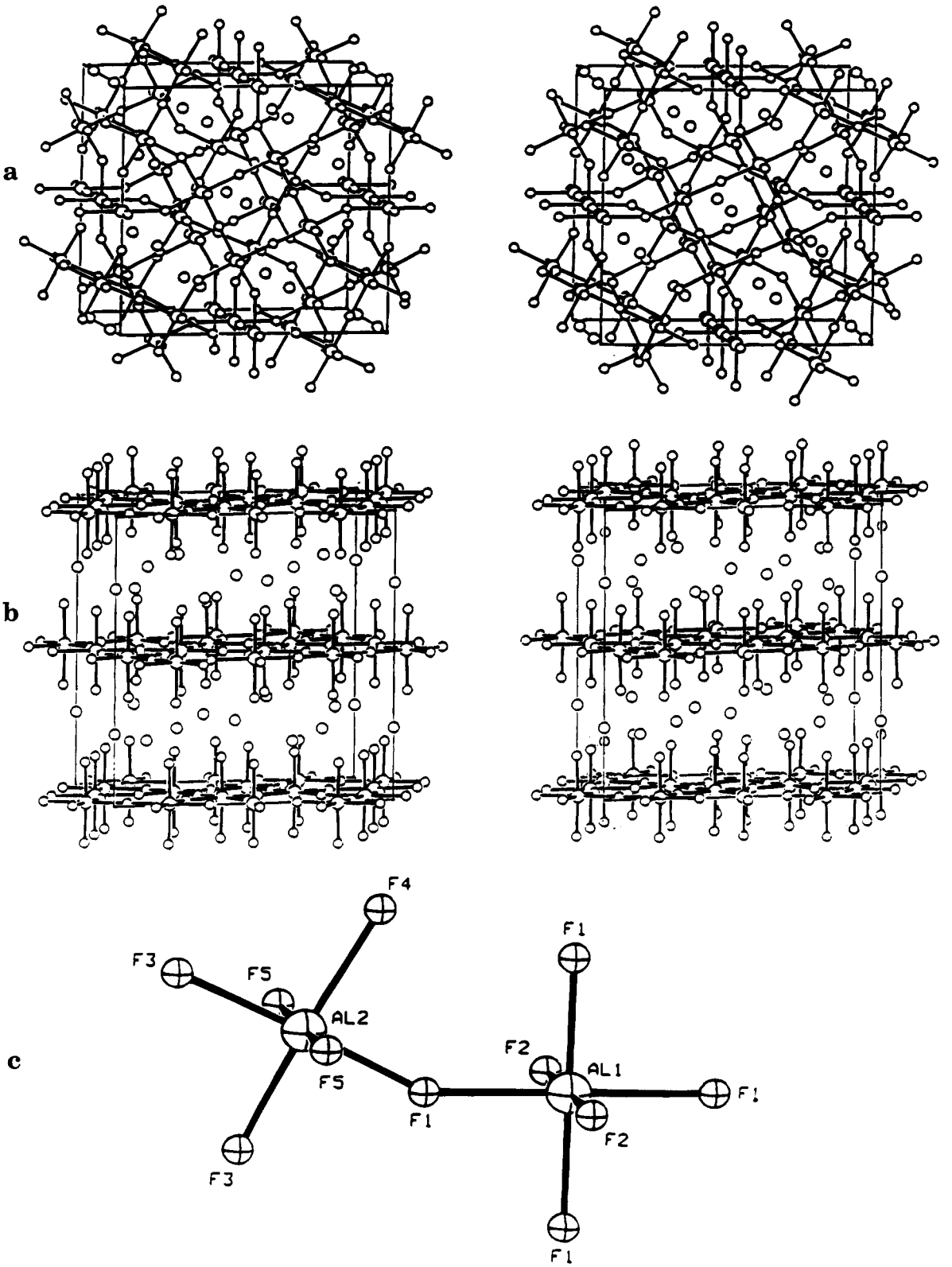

Figure 5. Structure of β-NH_4AlF_4 with (a) stereoview approximately parallel to the c axis; the 4-rings (center) are stacked one on top of another but are staggered from one layer to the next. The 3- and 5-ring pair in one layer sit above/below a 5- and 3-ring pair in the adjacent layers. (b) Stereoview approximately perpendicular to the c axis. (c) The atom labeling scheme for β-NH_4AlF_4.

to any previously known structural phase of AlF_3. We designated this second new phase θ-AlF_3, and the structure was elucidated by combined XRD and neutron powder diffraction analysis. Since our original solution of the structure, another report of this same structural phase, designated **t**-AlF_3 by Bentrup et al.,[13] has appeared. Their structure and ours are essentially identical. The structure is depicted in Figure 4a,b and, as one expects, again consists of corner-shared [AlF_6] octahedra. The tetragonal unit cell has four independent Al and seven independent F atoms assembled into rings of five, four, and three [AlF_6] octahedra. The 5-rings [a new structural motif for pure AlF_3 phases, although it has been found in $RbAlF_4$[14,15]] form an

Table 3

(a) Positional and Isotropic Thermal Parameters for β-NH_4AlF_4

atom	multiplicity, Wyckoff letter, site sym		X	Y	Z	U_{iso}
Al(1)	4 d	*m.mm*	0.5	0.0	0.0	0.021(3)
Al(2)	16 k	*m..*	0.2077(4)	0.0736(4)	0.0	0.012(1)
F(1)	16 k	*m..*	0.3412(5)	0.0005(4)	0.0	0.021(2)
F(2)	8 g	2.*mm*	0.5	0.0	0.1358(7)	0.028(3)
F(3)	16 k	*m..*	0.1412(4)	−0.0668(6)	0.0	0.025(2)
F(4)	8 h	*m*.2*m*	0.2842(4)	0.2158(4)	0.0	0.026(3)
F(5)	32 m	1	0.2057(4)	0.0778(4)	0.1396(3)	0.028(1)
N(1)[a]	16 l	..*m*	0.3386(4)	−0.1615(4)	0.1997(5)	0.116(6)
N(2)[a]	4 a	422	0.0	0.0	0.25	0.109(10)

(b) Bond Distances (Å) and Angles (deg) for β-NH_4AlF_4

atoms	no.	bond	atoms	no.	bond
Al(1)−F(1)	4	1.848(6)	N(1)− −F(1)	2	3.154(6)
Al(1)−F(2)	2	1.719(9)	N(1)− −F(2)	1	2.779(7)
Al(2)−F(1)	1	1.771(6)	N(1)− −F(4)	1	3.236(7)
Al(2)−F(3)	1	1.809(7)	N(1)− −F(5)	2	3.275(5)
Al(2)−F(3)	1	1.819(7)	N(1)− −F(5)	2	3.170(7)
Al(2)−F(4)	1	1.879(5)	N(1)− −F(5)	2	2.734(6)
Al(2)−F(5)	2	1.769(4)	N(2)− −F(5)	1	2.916(4)

atoms	no.	angle	atoms	no.	angle
F(1)−Al(1)−F(1)	2	180.0	F(1)−Al(2)−F(5)	2	91.5(3)
F(1)−Al(1)−F(1)	2	89.6(3)	F(3)−Al(2)−F(3)	1	90.3(4)
F(1)−Al(1)−F(1)	2	90.4(3)	F(3)−Al(2)−F(4)	1	177.1(4)
F(1)−Al(1)−F(2)	8	90.0	F(3)−Al(2)−F(4)	1	92.6(4)
F(2)−Al(1)−F(2)	1	180.0	F(3)−Al(2)−F(5)	2	91.1(2)
F(1)−Al(2)−F(3)	1	86.6(3)	F(3)−Al(2)−F(5)	2	88.6(3)
F(1)−Al(2)−F(3)	1	176.9(4)	F(4)−Al(2)−F(5)	2	89.0(2)
F(1)−Al(2)−F(4)	1	90.5(4)	F(5)−Al(2)−F(5)	1	176.5(5)
Al(1)−F(1)−Al(2)		151.5(3)	F(2)− −N(1)− −F(5)	2	111.0(2)
Al(2)−F(3)−Al(2)		179.7(1)	F(5)− −N(1)− −F(5)	2	81.4(3)
Al(2)−F(4)−Al(2)		146.5(6)			

[a] Occupancies were allowed to refine to account for disordered hydrogen atom contributions: N(1), 1.54(2); N(2), 1.45(2). See Figure 5c for labeling scheme.

Table 4

(a) Positional and Isotropic Thermal Parameters[a] for κ-AlF_3

atom	multiplicity, Wyckoff letter, site sym		X	Y	Z	U_{iso}[a]
Al(1)	8 i	*m..*	0.4205(3)	0.2928(2)	0.0	0.0126(6)
Al(2)	2 d	*m.mm*	0.5	0.0	0.0	0.0126(6)
F(1)	8 i	*m..*	0.3585(2)	0.4333(3)	0.0	0.0026(6)
F(2)	8 i	*m..*	0.5049(2)	0.1568(3)	0.0	0.0026(6)
F(3)	8 j	*m..*	0.4264(3)	0.2950(3)	0.5	0.0251(9)
F(4)	4 g	*m*.2*m*	0.2838(3)	0.2162(3)	0.0	0.0026(6)
F(5)	2 c	*m.mm*	0.5	0.0	0.5	0.0251(9)

(b) Bond Distances (Å) and Angles (deg) for κ-AlF_3

atoms	no.	bond	atoms	no.	bond
Al(1)−F(1)	2	1.828(4)	Al(2)−F(2)	4	1.789(3)
Al(1)−F(2)	1	1.825(4)	Al(2)−F(5)	2	1.772(1)
Al(1)−F(3)	2	1.773(4)			
Al(1)−F(4)	1	1.787(3)			

atoms	no.	angle	atoms	no.	angle
F(1)−Al(1)−F(1)	1	89.6(2)	F(2)−Al(1)−F(4)	1	92.5(2)
F(1)−Al(1)−F(2)	1	82.4(2)	F(3)−Al(1)−F(3)	1	175.4(3)
F(1)−Al(1)−F(2)	1	172.0(2)	F(3)−Al(1)−F(4)	2	92.3(2)
F(1)−Al(1)−F(3)	2	87.0(2)	F(2)−Al(2)−F(2)	2	93.6(2)
F(1)−Al(1)−F(3)	2	90.1(2)	F(2)−Al(2)−F(2)	2	86.4(2)
F(1)−Al(1)−F(4)	1	174.9(3)	F(2)−Al(2)−F(2)	2	180.0
F(1)−Al(1)−F(4)	1	95.5(2)	F(2)−Al(2)−F(5)	8	90.0
F(2)−Al(1)−F(3)	2	89.5(2)	F(5)−Al(2)−F(5)	1	180.0
Al(1)−F(1)−Al(1)		179.6(2)	Al(1)− −F(4)− −Al(1)		148.6(3)
Al(1)−F(2)−Al(2)		146.4(2)	Al(2)− −F(5)− −Al(2)		180.0
Al(1)−F(3)−Al(1)		175.4(3)			

[a] The thermal parameters of the two aluminum atoms were constrained to be equivalent, as were those of the three in-plane fluorine atoms and the two out-of-plane fluorine atoms. See Figure 6c for labeling scheme.

undulating 3-D interconnected channel system around tetrahedral clusters of four [AlF_6] octahedra—this latter feature being identical to that found in the pyrochlore η-phase above and indicating a close structural relationship between the two phases. The Al−F bond lengths range from 1.738(5) to 1.862(2) Å; the *cis*- and *trans*-F−Al−F angles are all within 3° of 90.0 and 180.0, respectively; the Al−F−Al angles vary from 140.2(2) to 180.0° (details are in Table 2).

(3) β-NH_4AlF_4 and κ-AlF_3. The appearance of the material $HAlF_4$ in the preparation of η-AlF_3 was intriguing, and we sought to prepare macrocrystalline samples for crystallography. An approach which suggested itself was to attempt to dissolve the pyridineH·AlF_4 precursor material into some high boiling point solvent, heat it in an inert atmosphere to boil out the pyridine and allow the $HAlF_4$ material to crystallize from the cooled solution. One solvent which proved viable for this approach was formamide, which was an excellent solvent for the pyridinium salt. Heating to 180 °C, a concentrated solution of the pyridinium salt begins to boil and fizz vigorously, whereupon a clear solid begins to precipitate. On cooling, a copious white precipitate forms and may be collected for XRD. The solid is microcrystalline, but the XRD is unlike the expected $HAlF_4$ phase. After detailed TGA, chemical and XRD analysis it was clear that the material was in fact of stoichiometry NH_4AlF_4 formed via. attack of the fluoroaluminate upon the formamide solvent itself in a manner similar to

$$\text{pyridineH.AlF}_4 + \text{HCONH}_2 \rightarrow \text{pyridine} + \text{CO} + \text{NH}_4\text{AlF}_4 \quad (1)$$

However, the XRD pattern was unlike that previously reported for NH_4AlF_4,[6] and detailed Reitveld analysis reveals the structure to be a new phase, β, of this material. The structure has a layered motif wherein sheets of corner-linked [AlF_6] octahedra are connected to form 3-, 4-, and 5-rings in a manner depicted in Figure 5. Between these layers reside the highly disordered ammonium cations. While similar to the known α-phase[6] (in that the structure is composed of sheets of corner-shared [AlF_6] octahedra sandwiched with ammonium ions), the connectivity within the sheets is very different. The registry between sheets is also different with adjacent layers having the five- and three-membered rings overlaid on one another. Overall, the structure is very similar to the β-phase structure of $RbAlF_4$.[15] Positional, bond length, and angle data are listed in Table 3.

It is interesting to note that if the synthesis of the NH_4AlF_4 material in formamide is conducted in a manner slightly different from that described in the

(13) Bentrup U. *Eur. J. Solid State Inorg.Chem.* **1992**, *t.29*, 51. LeBail, A.; Fourquet, J. L.; Bentrup, U. *J. Solid State Chem.* **1992**, *100*, 151.
(14) Brosset, C. *Z. Anorg. Allg. Chem.* **1938**, *239*, 301. Losch, R.; Hebecker, C. *Z. Naturforsch.* **1979**, *34B*, 131.
(15) Fourquet, J. L.; Plet, F.; DePape, R. *Acta Crystallogr.* **1980**, *B36*, 1997.

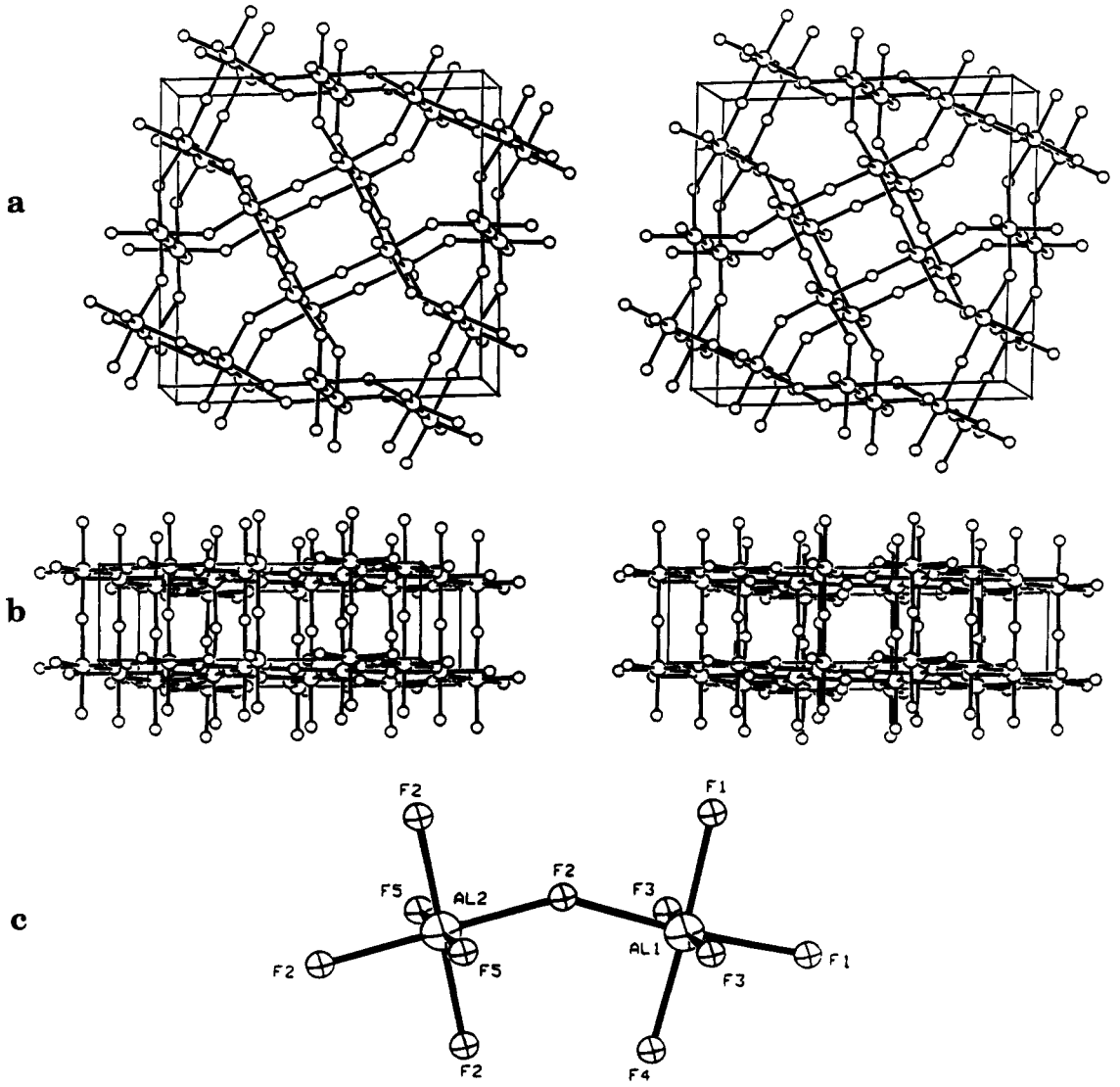

Figure 6. (a) Stereoview of κ-AlF_3 viewed approximately perpendicular to the *ab* plane. (b) Stereoview approximately perpendicular to the *c* axis. (c) The atom labeling scheme for κ-AlF_3.

Experimental Section—namely, where the pyridineH·AlF_4 solution in formamide is boiled for a prolonged period (15 min) rather than for ~1 min—the product is still NH_4AlF_4 but now in the previously reported α-NH_4AlF_4 phase. Likewise, taking our new β-phase material and reslurrying it into fresh formamide and reboiling for extended periods leads to its conversion into the α-phase. This implies that the β-phase of NH_4AlF_4 is a metastable form which can readily convert into the more thermodynamically stable α-phase in the presence of formamide solvent. However, heating the dry solid of α-NH_4AlF_4 to 450 °C gives the previously reported β-AlF_3, whereas heating the dry β-NH_4AlF_4 gives the new κ-AlF_3 as now described.

TGA of this new phase, β-NH_4AlF_4 shows a single weight-loss event at 350–400 °C corresponding to loss of NH_4F (Figure 2c) and the product AlF_3 has an XRD which is clean and is again a new phase which we designate κ. Detailed Reitveld analysis of the powder diffraction data reveals a structure which is depicted in Figure 6a,b. This structure is derived from the precursor ammonium salt by retaining the layer connectivity but eliminating NH_4F from between the layers, bringing the layers into perfect registry (i.e., 5-rings are now lined up over 5-rings, etc.) and then fusing the layers together via Al–F–Al linkages. This is, therefore, referred to as a pseudotopotactic transformation in that the layer structure of the precursor is maintained. The structure has linear channels running through the crystal comprised of 5-, 4-, and 3-rings of corner-shared [AlF_6] octahedra. Details of the structure along with bond length and angle data are in Table 4.

The structure bears many similarities to that of the hypothetical end member of the series of tetragonal tungsten bronzes K_xWO_3 where $x = 0$.[16] In that case the network of octahedra are all [WO_6] units, but their connectivity is identical to our [AlF_6] units producing the same three-, four-, and five-membered ring channels. In the potassium ion containing bronzes the alkali metal ions reside in these channels whereas in our structure these channels appear to be empty.

(4) Properties of New Phases. An estimate of the openness of these three new structures may be revealed by calculation of the cell volume per formula unit (VFU). Such calculation reveals VFU's of $\alpha = 43.6$, $\kappa = 46.1$, $\theta = 46.5$, $\beta = 49.4$, $\eta = 55.7$ Å^3, indicating a progressively less-dense structure through this series. Surface area

(16) Wells, A. F. In *Structural Inorganic Chemistry*, 5th ed.; Clarendon Press: Oxford, 1986; pp 613–615.

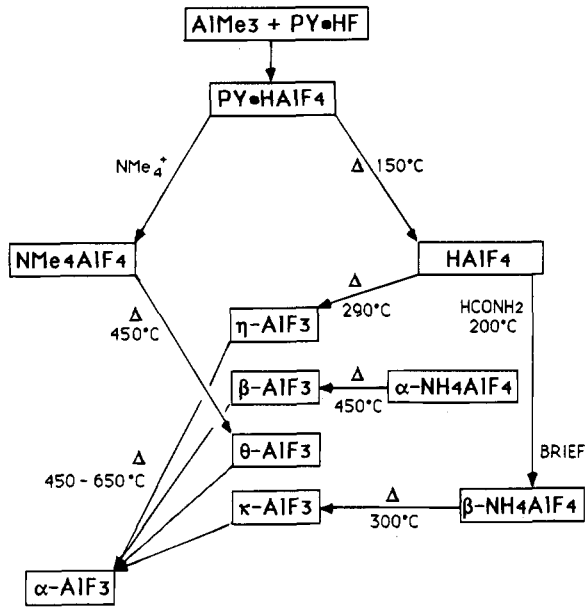

Figure 7. Summary scheme of synthetic routes to new Al–F species.

assessment, by BET nitrogen absorption, reveals surface areas of $\eta = 58$, $\theta = 64$, and $\kappa = 19$ m^2/g—these areas representing the external surface area of the crystallites with no contribution from the nanoporous openings present within the crystal lattice itself since nitrogen is too large to access these pores.

Finally, with three new phases of AlF_3 in hand, we have sought to establish their relationship to previous phases by examining their thermal transformations as followed by in situ XRD and DSC. We find that all three new phases transform directly and irreversibly in an exothermic event to the α-phase at temperatures around 450–650 °C—behavior which mimics that of the previously known β-phase: $\eta \rightarrow \alpha$, 450 °C; $\theta \rightarrow \alpha$, 610 °C; $\kappa \rightarrow \alpha$, 640 °C; $\beta \rightarrow \alpha$, 660 °C (all transitions are ~50–100 °C broad, centered at temperatures indicated). It is clear that while the α-phase is the thermodynamically most stable, the β-, η-, θ-, and κ-phases do not interconvert among themselves. There is, therefore, no structural progression through these phases en route to α.

Conclusions

The newly developed synthetic and phase chemistry of the fluoroaluminate species reported in this paper is summarized in Figure 7. The previously reported[7,12] organic cation salts of AlF_4 species provide new routes to what is clearly a rich phase chemistry of AlF_3. The phase of AlF_3 produced in any given synthesis is apparently dictated by the temperature of synthesis and especially by the precursor from which it is made. In the case of our syntheses from organic cation salts of the $R^+AlF_4^-$ formulation, we find a correlation between the intermediacy of an $HAlF_4$ material during the thermal decomposition and the phase produced. When the $HAlF_4$ intermediate forms as a discrete phase, we invariably produce η-AlF_3 as the major product whereas if no such intermediate is formed, θ-AlF_3 is the major product. These intriguing observations have prompted us to begin structural investigations of the solid acid $HAlF_4$ in the hope that some structural feature of this material will explain its intermediacy en route to the η-phase AlF_3 . The κ-phase appears to be uniquely produced from the new β-NH_4AlF_4 phase by a pseudotopotactic fusion process described above.

Acknowledgment. We thank Dr. Richard Li for electron diffraction work, Dr. W. E. Farneth for TGA-MS, J. B. Jensen, L. Ayers, and P. Pulcher for technical assistance. J.B.P. is grateful to DuPont and NSF Grant DMR-90-24249 for financial support. The authors are grateful to the Department of Energy for their general support of the neutron and synchrotron facilities at Brookhaven (HFBR and NSLS) and Oak Ridge (HFIR) and for their direct support of the beamlines mentioned in this paper. We would also like to thank our colleagues at these facilities: D. Cox and J. Hriljac for their operation of NSLS beamline X7a and for their technical expertise in ab initio structure determinations. We also owe thanks to P. Stephens (SUNY, Stoneybrook) for bringing up the new powder station at X3b1 in a timely fashion. The work at the NSLS, Brookhaven National Laboratory, was supported by the Division of Materials Sciences and Division of Chemical Sciences, U.S. Department of Energy. The work at Oak Ridge was supported by the Division of Material Sciences, U.S. Department of Energy, under Contract DE-AC05-84OR21400 with Martin Marietta Energy Systems, Inc. We also wish to thank Q. Huang from NIST for collecting the original pattern on the κ-AlF_3 form, which suggested that there might be extra hydrogen still in the material. We are grateful to one of the referees, who pointed out the relationship between our κ-AlF_3 and the tetragonal tungsten bronzes.

Supplementary Material Available: XRD and neutron diffraction patterns and their fits to the structural models for η- and θ-AlF_3 and β-NH_4AlF_4 (6 pages). Ordering information is given on any current masthead page.

CM940445K